Japanese Journal of Applied Physics
Vol. 46, No. 1, 2007, pp. 286–288

©2007 The Japan Society of Applied Physics

Brief Communication

Acoustic Imaging of Ferroelectric Domains in $BaTiO_3$ Single Crystals Using Atomic Force Microscope

Huarong ZENG*, Kiyoshi SHIMAMURA, Chinna Venkadasamy KANNAN, Encarnacion G. VILLORA, Shunji TAKEKAWA, Kenji KITAMURA, and Qingrui YIN[1]

Optronic Materials Center, National Institute for Materials Science, 1-1 Namiki, Tsukuba, Ibaraki 305-0044, Japan
[1]*Shanghai Institute of Ceramics, Chinese Academy of Sciences, 1295 Dingxi Road, Shanghai 200050, People's Republic of China*

(Received August 3, 2006; accepted October 3, 2006; published online January 10, 2007)

An "alternating-force-modulated" atomic force microscope (AFM) operating in the acoustic mode, generated by launching acoustic waves on the piezoelectric transducer that is attached to the cantilever, was used to visualize the ferroelectric domains in barium titanate ($BaTiO_3$) single crystals by detecting acoustic vibrations generated by the tip and transmitted through the sample placed beneath it to the transducer. The acoustic signal was found to reflect locally elastic microstructures at low frequencies, while high-frequency acoustic images revealed strip like domain configurations of internal substructures in $BaTiO_3$ single crystals. The underlying acoustic imaging mechanism using the AFM was discussed in terms of the interaction between the excited acoustic wave and ferroelectric domains. [DOI: 10.1143/JJAP.46.286]

KEYWORDS: $BaTiO_3$ single crystal, ferroelectric domain, atomic force microscopy, acoustic image

Nanoscale structures and physical properties are of fundamental interest, and thus variations in scanning probe microscopy techniques have been developed to understand nanoscale physical phenomena in basic research and potential technological applications.[1)] Very recently, scanning near-field ultrasound holography has been developed that provides nanoscale-resolution images of the internal substructures of microelectronic materials and malaria parasites in red blood cells.[2)] In the field of ferroelectrics, nanoscale domain structures of ferroelectric thin films, ceramics and single crystals can be imaged and controlled directly using piezoresponse force microscopy.[3–10)] Besides, acoustic mode scanning force microscopy including atomic force acoustic microscopy,[11,12)] ultrasonic force microscopy,[13–16)] and scanning probe acoustic microscopy[17–21)] have the advantage of visualizing nanoscale domain structures, elastic properties or subsurface configurations. In the present study, a type of alternating-force-modulated atomic force microscope (AFM) in the acoustic mode was developed by exciting acoustic waves on the piezoelectric transducer, which is fixed on a cantilever in the commercial AFM. This acoustic mode AFM was used to visualize the ferroelectric domains in $BaTiO_3$ single crystals.

An alternating force-modulated AFM, functioning in the acoustic mode, was set up by modifying a commercial AFM (SPA 400, SPI3800N, Seiko, Japan). A schematic sketch of the modified AFM is shown in Fig. 1. An external sinusoidal signal provided by a function generator (33120A, Agilent) was applied to the piezoelectric transducer attached to the cantilever, thereby inducing a periodical vibration in the cantilever/tip system. This modulated-tip vibration driven by the function generator emits a local stress field underneath the tip, resulting in an acoustic vibration inside the sample, which gives rise to a remarkable acoustic response of the ferroelectric microstructure due to physical phenomenal effects. The resultant acoustic signal carrying ferroelectric information was converted into an electrical signal through a piezoelectric lead zirconium titanate (PZT) ceramic transducer bonded onto the sample, and then fed to a lock-in amplifier (Model 7280 DSP, Signal Recovery Instrumentation) for detection. For the experiment, a 2-μm-thick 90-μm-long Ti/Pt-coated silicon cantilever (Micro Mash, NSC12-B) with a spring constant of 14 N/m and a resonance frequency of 315 kHz was used. For the present study, we chose a 0.3-mm-thick (001)-oriented $BaTiO_3$ single crystal.

Figures 2(a) and 2(b) are a topography image and the corresponding acoustic image of a $BaTiO_3$ single crystal, respectively, at a modulation frequency of 133.42 kHz. It can be clearly seen that the acoustic features are nearly the same as those of the topography image, indicating only slight variations in the surface microstructure after sample polishing. Figure 2(c) shows an acoustic image taken at a frequency of 1.419 MHz in the same scanning area. Unlike Fig. 2(b), a different acoustic response is clearly seen in Fig. 2(c), exhibiting remarkable acoustic contrasts in parallel strips about 300 nm in width, which are obviously the 90° ferroelectric domains in the $BaTiO_3$ single crystal. The striped patterns are more distinguished in another large scanning area of $10 \times 10\,\mu m^2$ measured at a frequency of 1.419 kHz, as shown in Fig. 3. The intercrossing domain phenomena shown in Fig. 3(b) reflect the domain state distribution at different depths throughout the specimen. Such phenomena were observed in Han and Cao's studies of the averaged domain configurations using a polarized optical microscope, in which the domain configurations at various depths were exhibited in an optical image by adjusting the focus.[22)]

In addition, internal defects with deep black contrasts inside the crystal also appear in the acoustic image, as indicated by arrows in Fig. 3(b), but which are not shown in the corresponding topography image in Fig. 3(a). The ferroelectric domain configuration in the acoustic images [Figs. 2(c) and 3(b)] could be further substantiated by non destructive scanning electron acoustic microscopy (SEAM), in which a periodically chopped electron beam consisting of a pair of deflection plates, an electron beam blanking power, a signal generator, a PZT and a lock-in amplifier is attached to a conventional scanning electron microscope (SEM; KYKY-1000B). The frequency-modulated periodically chopped electron beam produces acoustic waves through the sample that are detected with a piezoelectric transducer

*E-mail address: zeng.huarong@nims.go.jp

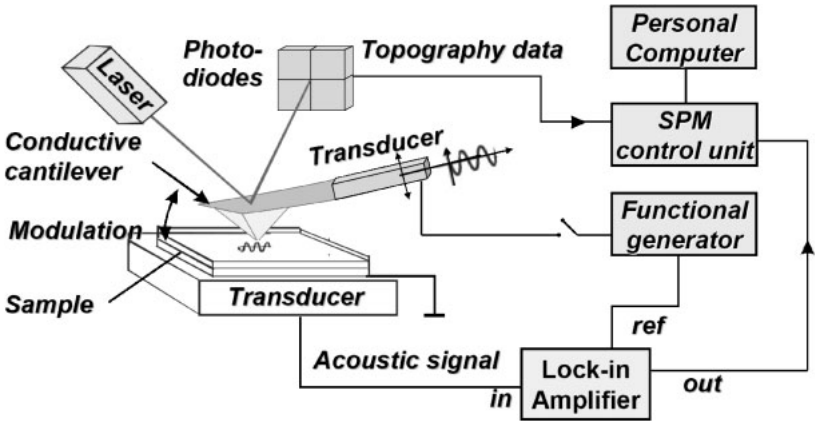

Fig. 1. Schematic diagram of AFM-based acoustic probe microscopy.

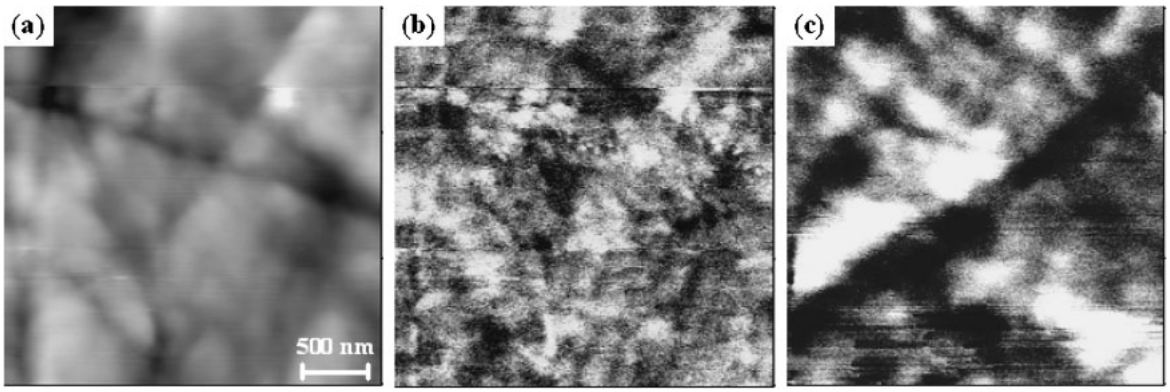

Fig. 2. Topography image (a) and corresponding acoustic images (b) and (c) of $3.0 \times 3.0\,\mu m^2$ scanning area in $BaTiO_3$ single crystal at modulation frequencies of 133.42 kHz and 1.419 MHz, respectively.

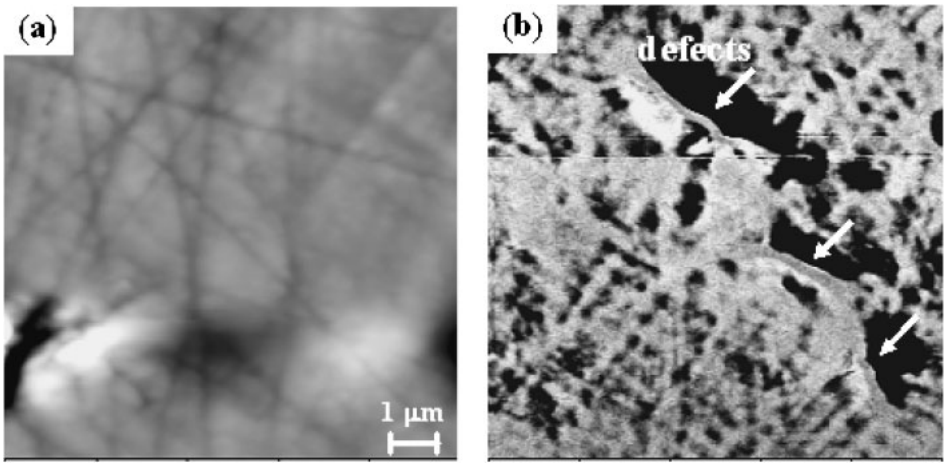

Fig. 3. Topography image (a) and corresponding acoustic image (b) of another large scanning area ($10 \times 10\,\mu m^2$) in $BaTiO_3$ single crystal at modulation frequency of 1.419 kHz.

coupled to the sample. In SEAM, spatial variations or discontinuities in any of these thermal and elastic properties produce contrast in the electron acoustic image. A secondary electron image (topography image) and a electron acoustic image (domain image) are simultaneously obtained in SEAM.[23] An acoustic image obtained with the same $BaTiO_3$ single crystal using SEAM is given in Fig. 4. As can be seen, the parallel domain pattern is observed in the acoustic SEAM image, although the domain widths are larger than those in Figs. 2(c) and 3(b), which is due to the lower resolution of SEAM than that of the present acoustic probe technique based on the AFM. According to Liu's high-resolution scanning probe acoustic microscopy studies, the ferroelectric domains in the $BaTiO_3$ single crystal demonstrate a typical hierarchy character.[24] Therefore, the AFM-based acoustic images of ferroelectric domains in Figs. 2(c) and 3(b) reveal finer substructure than those obtained with SEAM.

The above phenomena and the origin of the acoustic contrasts in the ferroelectric $BaTiO_3$ single crystal under an

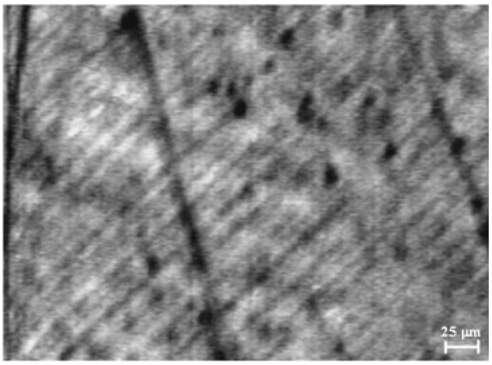

Fig. 4. Electron acoustic image of ferroelectric domains in $BaTiO_3$ single crystal obtained using scanning electron acoustic microscope.

alternating force can be conceptually understood from the point of view of the interaction between the excited acoustic waves and the microstructures in the specimen. In AFM-based acoustic imaging, the local acoustic vibration excited by the periodical tip force, as a primary acoustic wave, propagates through the $BaTiO_3$ single crystal sample and interacts with the ferroelectric domain structures, because the bulk electric polarization influences the elastic response of a ferroelectric material when stresses are applied.[25] Consequently, a secondary acoustic wave arising from such an interaction, bearing the physical properties of a ferroelectric domain, transmits from the bottom side of the sample and penetrates into the PZT-type piezoelectric transducer, in which the secondary acoustic wave will induce an in-phase thick-mode piezoelectric vibration, provided that the excited frequency is close to the thick vibration frequency of the piezoelectric transducer, followed by the output polarization orientation-carrying acoustic signal due to normal piezoelectric effects. Suppose that the excited frequency is far lower than the thick vibration frequency of the PZT-type piezoelectric transducer; clearly, it is extremely difficult to excite and detect the acoustic signal related to the ferroelectric domains. Moreover, in our acoustic mode AFM unit, the PZT-type transducer had a thick vibration frequency of 1.432 kHz, according to the frequency spectrum, which helped us to clearly visualize the ferroelectric domain in the $BaTiO_3$ crystal at a high frequency of 1.419 MHz [Figs. 2(c) and 3(b)], but not in the case of low frequencies. Only surface microstructures could be observed in the latter case [Fig. 2(b)]. The domain contrasts in the acoustic image at high frequency are owing to the different elastic properties between the c-domain and the a-domain. Since ferroelectric domains with different polarization orientations have different elastic constants, an elastic response appearing in the acoustic image for an individual domain would be different.[25] Thus, only a non-180° domain (i.e., ferroelastic domain) can lead to such elastic response phenomena for the acoustic wave in the sample, while antiparallel ferroelectric domains undoubtedly have similar acoustical signals and imaging contrasts, but are not distinguishable in an acoustic image. As a result, only 90° domains appear in the acoustic image of the $BaTiO_3$ single crystal at high frequencies, as evidently shown in Figs. 2(c) and 3(b).

In summary, an alternating force-modulated AFM operating in acoustic mode was used to enable a frequency-modulated alternative voltage on a cantilever bimorph based on a commercial AFM, thereby visualizing ferroelectric domains in a $BaTiO_3$ single crystal by detecting acoustic vibrations generated by the tip and transmitted through a sample placed beneath the transducer. It was found that in the case of low frequency, locally elastic microstructures occur in the acoustic image, while high-frequency acoustic images revealed strip like domain configurations of internal substructures in the $BaTiO_3$ single crystal. The acoustic imaging mechanism for ferroelectric domains was related to the interaction between the excited acoustic vibration and ferroelectric domains, and the thick vibration mode of the piezoelectric transducer at high frequencies.

1) J. Loos: Adv. Mater. **17** (2005) 1821.
2) G. S. Shekhawat and V. P. Dravid: Science **310** (2005) 89.
3) A. Gruverman, O. Auciello, and H. Tokumoto: Annu. Rev. Mater. Sci. **28** (1998) 101.
4) V. Nagarajan, A. Roytburd, A. Stanishievskv, S. Prasertchoung, T. Zhao, L. Chen, J. Melngailis, O. Auciello, and R. Ramesh: Nat. Mater. **2** (2003) 43.
5) M. Molotskii, A. Agronin, P. Urenski, M. Shvebelman, G. Rosenman, and Y. Rosenwaks: Phys. Rev. Lett. **90** (2003) 107601.
6) K. Terabe, M. Nakamura, S. Takezawa, K. Kitamura, S. Higuchi, Y. Gotoh, and Y. Cho: Appl. Phys. Lett. **82** (2003) 433.
7) S. V. Kalinin: Phys. Rev. B **70** (2004) 184101.
8) F. M. Bai, J. F. Li, and D. Viehland: Appl. Phys. Lett. **85** (2004) 2313.
9) D. Scrymgeour and V. Gopalan: Phys. Rev. B **72** (2005) 024103.
10) P. Paruch, T. Giamarchi, and J.-M. Triscone: Phys. Rev. Lett. **94** (2005) 197601.
11) U. Rabe, M. Kopycinska, S. Hirsekorn, J. M. Saldana, G. A. Schneider, and W. Arnold: J. Phys. D **35** (2002) 2621.
12) D. C. Hurley, M. Kopycinska-Muller, A. B. Kos, and R. H. Geiss: Meas. Sci. Technol. **16** (2002) 2167.
13) T. Tsuji, H. Ogiso, J. Akedo, S. Saito, K. Fukuda, and K. Yamanaka: Jpn. J. Appl. Phys. **43** (2004) 2907.
14) O. V. Kolosov, M. R. Castell, C. D. Marsh, G. A. D. Briggs, T. I. Kamins, and R. S. Williams: Phys. Rev. Lett. **81** (1998) 1046.
15) K. Inagaki, O. V. Kolosov, G. A. D. Briggs, and O. B. Wright: Appl. Phys. Lett. **76** (2000) 1836.
16) O. Matsuda, T. Terada, K. Inagaki, and O. B. Wright: Jpn. J. Appl. Phys. **41** (2002) 3545.
17) X. X. Liu, R. Heiderhoff, H. P. Abicht, and L. J. Balk: J. Phys. D **35** (2002) 74.
18) X. X. Liu, R. Heiderhoff, H. P. Abicht, and L. J. Balk: Anal. Sci. **17** (2001) S57.
19) Q. R. Yin, G. R. Li, H. R. Zeng, X. X. Liu, R. Heiderhoff, and L. J. Balk: Appl. Phys. A **78** (2004) 699.
20) H. R. Zeng, H. F. Yu, S. X. Hui, R. Q. Chu, G. R. Li, H. S. Luo, and Q. R. Yin: Solid State Commun. **133** (2005) 521.
21) H. R. Zeng, H. F. Yu, L. N. Zhang, R. Q. Chu, G. R. Li, and Q. R. Yin: Phys. Status Solidi A **202** (2005) R41.
22) J. Han and W. Cao: Appl. Phys. Lett. **83** (2003) 2040.
23) B. Y. Zhang, F. M. Jiang, Q. R. Yin, and S. Kojima: J. Appl. Phys. **80** (1996) 1916.
24) X. X. Liu: Ph. D. thesis, Wuppertal University, Germany, 2001.
25) A. Moulson and J. M. Herbert: *Electroceramics* (Chapman and Hall, London, 1990) p. 353.